Molecular Crystals and Liquid Crystals

ISSN: 1542-1406 (Print) 1563-5287 (Online) Journal homepage: http://www.tandfonline.com/loi/gmcl20

Enhanced photovoltaic and carrier collection efficiency of dye sensitized solar cell: Nb_2O_5 coated TiO_2 photoanode

Bo Youn Jang, Ji Young Park, Ji Won Lee, Rajesh Cheruku & Jae Hong Kim

To cite this article: Bo Youn Jang, Ji Young Park, Ji Won Lee, Rajesh Cheruku & Jae Hong Kim (2016) Enhanced photovoltaic and carrier collection efficiency of dye sensitized solar cell: Nb_2O_5 coated TiO_2 photoanode, Molecular Crystals and Liquid Crystals, 635:1, 139-147, DOI: 10.1080/15421406.2016.1200399

To link to this article: http://dx.doi.org/10.1080/15421406.2016.1200399

Published online: 01 Nov 2016.

MOLECULAR CRYSTALS AND LIQUID CRYSTALS
2016, VOL. 635, 139–147
http://dx.doi.org/10.1080/15421406.2016.1200399

Taylor & Francis
Taylor & Francis Group

Enhanced photovoltaic and carrier collection efficiency of dye sensitized solar cell: Nb_2O_5 coated TiO_2 photoanode

Bo Youn Jang, Ji Young Park, Ji Won Lee, Rajesh Cheruku, and Jae Hong Kim

School of Chemical Engineering, Yeungnam University, Dae-dong, Gyeongsan-si, Gyeongsangbuk-do, South Korea.

ABSTRACT

Dye sensitized solar cells (DSSCs) were fabricated using Nb_2O_5 energy barrier layer is coated on the TiO_2 photoanode. This energy barrier (Nb_2O_5 layer) reduces the recombination rate of the photoinjected electrons with their counter holes. A monoclinic Nb_2O_5 energy barrier layer can be coated 1 and 3 times on a TiO_2 photoanode using a dip-coating method. The Nb_2O_5/TiO_2 photoanode exhibits enhanced photovoltaic performance, which is better than the bare TiO_2 photoanode. The results presented in this study show that this Nb_2O_5 layer forms an inherent energy barrier at the electrode-electrolyte interface. The electron transport and charge recombination behaviors of DSSCs were investigated by electrochemical impedance spectra (EIS) and the results illustrated that the DSSCs showed the lowest charge transport resistance and the longest electron lifetime. The electron transport and recombination were studied by stepped light- induced transient measurements of photocurrent and voltage (SLIM-PCV) method and shown that the electron diffusion length is increasing with the Nb_2O_5 coating.

KEYWORDS

Nb_2O_5; Photoanode; Electron transport

1. Introduction

Dye-sensitized solar cells (DSSCs) are an alternative to the conventional silicon based solar cells because of their tunable optical assets, for instance, color and transparency, negligible environmental impact, low-cost, meek fabrication process, and environmental advantages [1–6]. DSSCs are generally composed of photoanode and the counter electrode (CE) separated by the redox pairs (I^-/I^{3-}) based electrolyte [7–9]. Photoanode is usually composed of a porous layer of TiO_2 nanoparticles deposited on fluorine-doped tin dioxide (FTO) sensitized by dye molecules, while the CE is generally FTO glass substrate coated with platinum (Pt) [7–9] and carbon nanostructures [10]. Since the evolution of first DSSCs, intensive amount of work has been done on the understanding of TiO_2 as photoanode. Although mesoporous TiO_2 shows the good result as a photoanode in DSSCs but it suffers from lower electron mobility and poor long term stability.

If the DSSC is illuminated with light, at that moment an electron is injected from the dye into the TiO_2 film followed by a hole transfer to the electrolyte [11, 12]. The injected electrons must cross the TiO_2 film and reach the conducting substrate, while the oxidized ions diffuse toward the back electrode where they are reduced again. The porous geometry that permits

CONTACT Rajesh Cheruku chraj25@ynu.ac.kr; Jae Hong Kim jaehkim@ynu.ac.kr
Color versions of one or more of the figures in the article can be found online at www.tandfonline.com/gmcl.

the presence of the electrolyte through the entire electrode provides a high surface area for recombination between the injected electrons and the holes in the solution [13, 14]. In the absence of an energy barrier at the electrode-electrolyte interface, the rate of this recombination process may be very high, depending on the properties of the hole carrier [11, 13, 15, 16]. For this reason, DSSCs using I^-/I^{3-} redox couple performs better than similar cells consisting of faster couples [17]. Furthermore, part of the low efficiencies observed with solid electrolytes are attributed to this recombination process. Therefore, the formation of an energy barrier at the surface of the TiO_2 electrode that will enable the use of various mediators has the prospect of improving DSSCs significantly.

The short circuit current density (J_{SC}) values of DSSCs with TiO_2 electrodes are determined by three factors, the light harvesting efficiency, the electron injection efficiency, and the electron collection efficiency. The light harvesting efficiency may be increased by increasing light absorption through dye loading or scattering. Previous studies have examined the application of various metal oxide shells such as SnO_2 [18], ZrO_2 [19], Nb_2O_5 [20–23], Al_2O_3 [19, 24, 25], and ZnO [26, 27] to TiO_2 electrodes. Mostly, the coating of each material layer forms an energy barrier that decreases the electron recombination losses, shifts the conduction band downward that increases the electron injection, or enhances the injection efficiency. This results in an increase in the J_{SC} and often accompany the increase in open-circuit voltage (VOC) as well.

This new electrode consists of an inner nanoporous TiO_2 matrix covered with a thin layer of Nb_2O_5. The conduction band potential difference of Nb_2O_5 is ca. 100 mV more negative than that of TiO_2 [27]. This potential difference can form an energy barrier at the electrode-electrolyte interface, thus reducing the rate of recombination of the photoinjected electrons and improving the collection efficiency. A comparison of two similar DSSCs that differ only in their nanoporous electrodes shows that the solar cells made from the new electrode are superior to cells containing the standard electrodes with respect to all parameters. Nb_2O_5 is such a promising metal oxide because it supports good N719 dye loading because of its basic character and its conduction band level is 100 meV higher than that of TiO_2 [27]. We report here for details of the preparation of this type of electrodes, the characterization of the electrode, and further evidence of the role of the coating on the electrode electrochemical behavior. In addition, the thickness of the Nb_2O_5 shell is controlled and the effect of its thickness on the photovoltaic performance is investigated.

2. Experimental details

2.1. Preparation of TiO_2 electrode

A conducting glass substrate (FTO; TEC8, Pilkington, 8 U/cm2, a thickness of 2.3 mm) was cleaned in ethanol under ultrasonication. A TiO_2 blocking layer was obtained by dipping FTO glass in a 0.04 M $TiCl_4$ aqueous solution at 70°C for 30 min. A TiO_2 paste was coated on an FTO substrate using the doctor-blade method, and the resulting coated substrate was sintered at 450°C for 30 min.

2.2. The deposition of Nb_2O_5 on TiO_2 electrode

The Nb_2O_5/TiO_2 nanorod electrodes were obtained using a dip-coating method. $Nb(OC_2H_5)_5$ was dissolved in 2-propanol (20 mM) to prepare the coating solution. TiO_2 electrodes were initially dipped into a coating solution for 10 seconds and taken out rapidly.

The resulting coated films were dried at room temperature and annealed at 500°C for 1 hour to yield the Nb_2O_5/ TiO_2 electrodes. The dip coating times were varied, 1 and 3 times.

2.3. Equipment and measurements

All electrodes were fabricated on fluorinated tin oxide glass substrates (TCO22–7, Solaronix) with a sheet resistance of 7 Ω-cm^2. The Nb_2O_5/TiO_2 electrodes were obtained using the dip-coating method. The linear sweep voltammetry experiments were conducted using a computer controlled potentiostat (IVIUMSTAT, IVIUM). Electrochemical impedance spectroscopy (EIS) was performed using an electronic-chemical analyzer (Iviumstat Tec.). The data were analyzed using Zview2 commercial software (Scribner Associates Inc.). The conductivity of the electrolyte system was derived from the complex impedance measurements. Pt-deposited FTO electrodes were used as both anode and cathode.

Transient measurements were performed by the same method as that reported by O'Regan et al. [28] and it is illustrated elsewhere [29]. A white light bias was generated from an array of diodes (Abet, LS Series light source) with red-light pulsed diodes (Thorlabs HNL210L system) as the perturbation source, controlled by a fast solid-state switch. The voltage dynamics were measured on a 1 GHz Tektronix oscilloscope (DPO4102B-L) across the high impedance (1 MΩ) port. The perturbation light source was set to a suitably low level such that the voltage decay kinetics were mono-exponential. Small perturbation transient photocurrent measurements were performed in a similar manner to the open-circuit voltage decay measurement. For the voltage decay measurements in the short-circuit regime, a Keithley 2600B source meter was connected in series with the solar cell and parallel with the oscilloscope which was set on the high impedance port. The Keithley sourced the current through the solar cell which was under bias illumination in such a way that the voltage was kept at 0 V (i.e., short-circuit). In this way, no extra current is allowed to flow through the device following the light pulse, therefore, the decay of the measured perturbation signal is entirely governed by the charge recombination within the cell. For the current decay measurements, while the charge is being collected the charges are also simultaneously recombining within the cell.

2.4. Assembly and characterization of DSSCs

A photosensitizer was loaded on the prepared anodes by immersing them in a 0.3 mM ethanol solution of N719 (Solaronix) at room temperature. The Pt counter electrodes were prepared by layering platinum paste (PT1, Dyesol Co.) on FTO glasses and annealing them at 450°C. These electrodes were assembled using a 60 μm-thick Surlyn (Dupont 1702) layer. The J-V characteristics of the prepared DSSCs were measured under 1 sunlight intensity (100 mW/cm^2, AM 1.5 G). Electrochemical impedance spectroscopy (EIS) measurements were carried out using a computer-controlled potentiostat (IVIUMSTAT, IVIUM).

3. Results and discussion

The photovoltaic performance of DSSCs is estimated from the current density-voltage (J-V) characteristics are examined for each DSSC under the illumination of AM 1.5 G solar simulated light and the corresponding results are shown in Fig. 1. The photovoltaic parameters of DSSCs are short circuit current density (J_{SC}), open circuit voltage (V_{OC}), fill factor (FF), and overall efficiency of power conversion (η) is summarized in Table 1. The J_{SC} and FF increase with increasing deposition times of Nb_2O_5 up to 1 and 3 times. An excessively thick layer

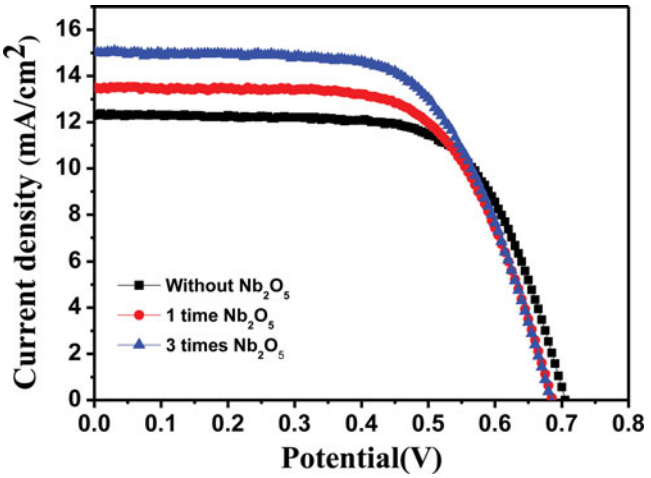

Figure 1. The current density-potential (J–V) curves for DSSC cells containing untreated TiO_2 and Nb_2O_5-coated TiO_2 electrodes, for different coating times.

of Nb_2O_5 reduces significantly the transfer rate of photo-generated electrons because the low conductivity of Nb_2O_5. V_{OC} tends to decrease with increasing deposition times. This indicates that an increase in deposition time leads to an increase in the number of defect sites, which is the center of charge recombination.

The differences in photocurrent density of these three solar cells were further investigated by measuring the incident photon-to-current efficiency (IPCE) spectra, as a function of wavelength, and the results are exhibited in Fig. 2. The photocurrent density Jsc and IPCE under each wavelength of radiation can be expressed by the following equations [30–32]:

$$\mathrm{Jsc}(\lambda) = q\eta_{\mathrm{IPCE}}(\lambda)\mathrm{I}_0 \tag{1}$$

$$\eta_{\mathrm{IPCE}}(\lambda) = \eta_{\mathrm{LH}}(\lambda)\eta_{\mathrm{CJ}}(\lambda)\eta_{\mathrm{CC}}(\lambda) \tag{2}$$

where q is the elementary charge, $\eta_{\mathrm{IPCE}}(\lambda)$ is the quantum efficiency under each light wavelength, I_0 is the illuminated light intensity, η_{LH} is the light-harvesting efficiency of a cell, $\eta_{\mathrm{CJ}}(\lambda)$ is the charge-injection efficiency and $\eta_{\mathrm{CC}}(\lambda)$ is the charge collection efficiency. The whole short circuit current can be obtained by integrating Eq. (1). High quantum efficiency means a high short current density. In our case, 1 and 3 times Nb_2O_5 coated on a TiO_2 photoanode exhibited a highest IPCE value than a bare TiO_2 photoanode and this phenomenon matched well with the J_{SC} results. The product of η_{LH}, η_{CJ}, and η_{CC} is commonly referred to the incident photon-to-current conversion efficiency as expressed in Eq. (2). Of the three parameters, η_{LH} is mainly determined by the amount of adsorbed dye, and η_{CJ} values of adsorbed N719 on

Table 1. Photovoltaic Parameters for DSSC cells Fabricated with Untreated TiO_2 and Nb_2O_5-Coated TiO_2 Electrodes, For Different coating times Tested under AM 1.5G 100 mW cm^{-2}.

Coating times of Nb_2O_5	J_{sc}($mAcm^{-2}$)	V_{oc}(V)	FF(%)	η(%)	R_{FTO}[a](Ω)	R_2[b](Ω)	R_3[c](Ω)
Untreated	12.30	0.702	65.55	5.69	18.81	3.67	13.85
1 time	13.06	0.680	63.04	5.84	17.93	3.47	13.50
3 times	15.03	0.677	61.41	6.31	20.46	2.78	12.78

[a] FTO Interface resistance
[b] Due to the resistance at the interface between the counter electrode and the electrolyte.
[c] Possibly originated from the backward charge transfer from TiO_2 to the electrolyte and the electron conduction in porous TiO_2 film.

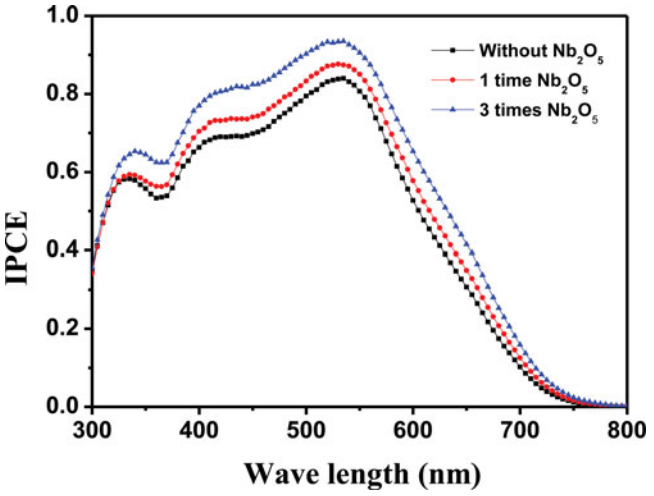

Figure 2. IPCE spectra of the condition for DSSC cells, containing untreated TiO_2 and Nb_2O_5-coated TiO_2, for different coating times.

the films can be assumed to be the same. So the performance of 1 and 3 times Nb_2O_5 coated DSSCs are compared to the bare TiO_2 photoanode.

To investigate the dramatic increase in J_{SC} for DSSCs prepared by increasing Nb_2O_5 in the Nb_2O_5-coated electrodes as compared to untreated TiO_2 that is an electron transport increase from the conduction band of TiO_2 to the electrolyte. EIS experiments are performed under illumination conditions by applying an ac voltage 10 mV and an AC frequency range between 100 kHz and 0.1 Hz to the dye sensitized photoanodes is shown in Fig. 3. These experiments provide useful information for understanding the charge recombination kinetics at the interfacial region between the photoanode and electrolyte.

The Nyquist plots in Fig. 3 revealed that the diameter of the semicircle tends to decrease with increasing deposition times of Nb_2O_5. This phenomenon is also depends on the rate of back-electron transfer at the TiO_2/electrolyte interface and the concentration of I_3^-. The

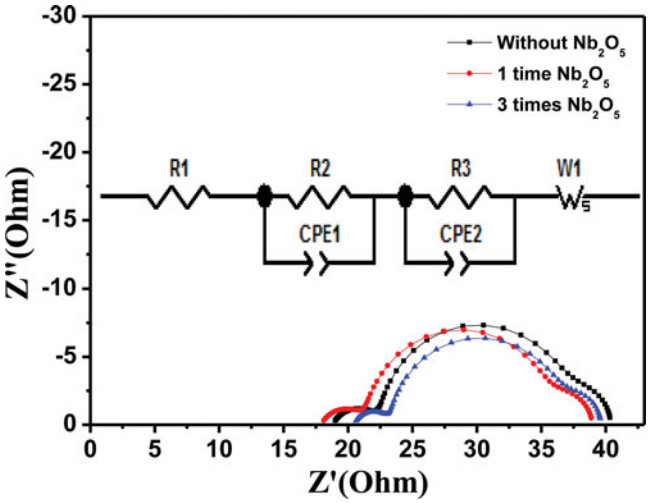

Figure 3. Electrochemical impedance spectroscopy (EIS) under illumination condition for DSSC cells containing untreated TiO_2 and Nb_2O_5-coated TiO_2, for different coating times.

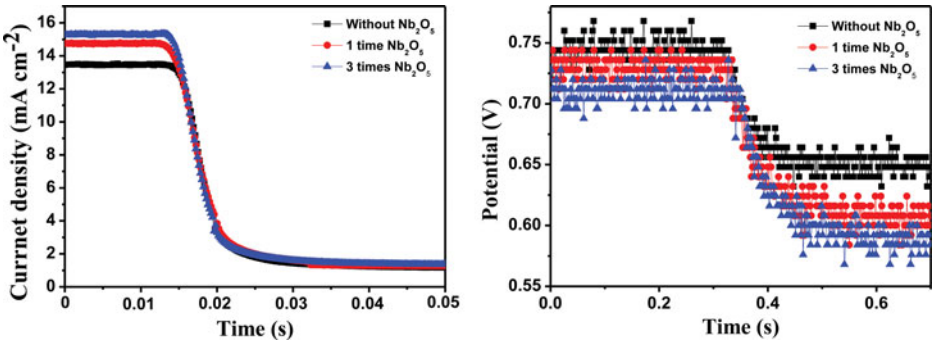

Figure 4. (a) Typical current responses of DSCs against the different stepped laser intensities. (b) Typical open circuit voltage transients induced by stepped laser intensity.

impedance spectrum was analyzed using an equivalent circuit for the TiO_2/electrolyte interface in the conductive state. The recombination resistance (R_3) was obtained by the curve of the large semicircle, as reported elsewhere [33]. In Table 1, the value of R_3 decreases for 1 and 3 times Nb_2O_5-coated as compared to untreated TiO_2 photoanode. This implies that the coating does not form a barrier layer to reduce the recombination loss. Moreover, a lowered degree of dye adsorption was observed on the Nb_2O_5-coated electrodes and the number of electrons generated by the adsorbed dye molecules on the Nb_2O_5-coated TiO_2 surface was not higher.

The enhancement of the electron injection might be attributed to the shift of the conduction band edge of TiO_2. Previously, it has been reported that the acidic property of Nb_2O_5 shifted the TiO_2 flat band energy potential (E_{fb}) toward positive values and increased the driving force for electron injection. This is determined as the difference between E_{fb} and the LUMO state of the dye, thereby enhancing the electron injection efficiency [34]. Thus, our results imply that the enhancement in the electron injection of TiO_2 electrodes due to the Nb_2O_5 coating improves the J_{SC} value.

Fig. 4 shows the photocurrent and the photovoltage response under stepped light was measured to quantify the carrier transport mechanism by calculating the diffusion coefficient and lifetime of photogenerated electrons. Fig. 5(a) presents the carrier diffusion coefficients of the pure and Nb_2O_5 coated photoanodes. The diffusion coefficient of the Nb_2O_5 coated photoanodes is not much different from that of pure photoanode. However, the Nb_2O_5 coated photoanodes has clearly changed the slope in the diffusion coefficient *vs.* short circuit current curves. The difference in slope manifests the existence of additional trapping sites via Nb_2O_5 coating, which significantly influences the carrier transport at different Fermi levels. The large diffusivity at larger short circuit current implies that Nb_2O_5 coated makes it easier for trapping and de-trapping of electrons under higher light flux. The smallest effective mass of electrons and the high ionization efficiency of Nb_2O_5 coating, reduce the chances for the trapping, leading to improved carrier transport [35, 36]. Fig. 5(b) shows the carrier lifetime of the Nb_2O_5 coated photoanodes. The 1 and 3 times Nb_2O_5 coated photoanodes exhibited longer lifetimes. As the short circuit current was increased (*i.e.* higher incoming light intensity), the difference in the lifetimes of the Nb_2O_5 coated photoanodes and pure photoanode increased. This improved lifetime is consistent with the results of EIS analysis, suggesting suppressed carrier recombination at the TiO_2-electrolyte interface.

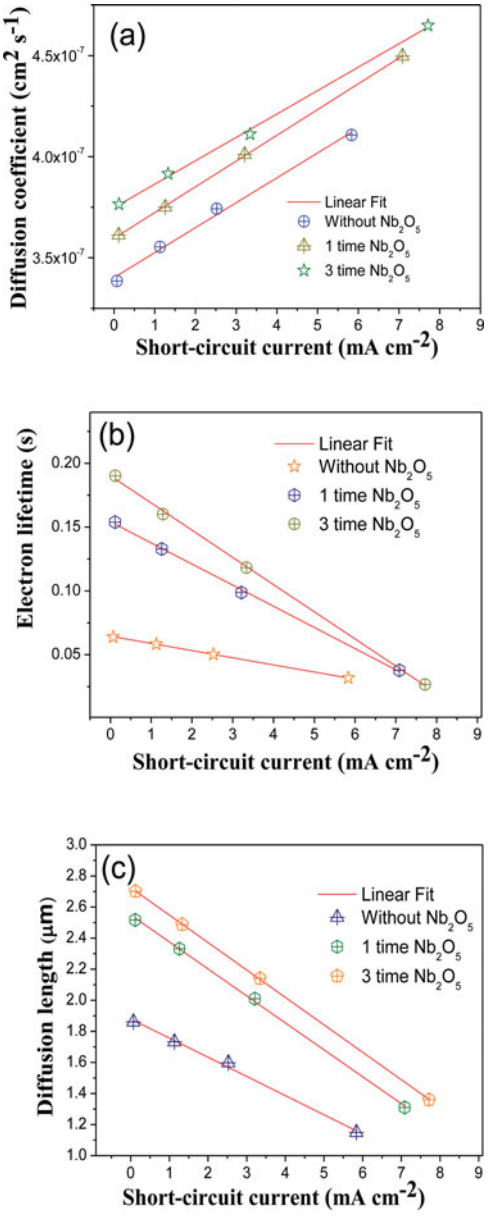

Figure 5. SLIM-PCV measurement of DSSCs **(a)** Diffusion coefficient, **(b)** electron lifetime, **(c)** electron diffusion length values vs short-circuit current of the DSCs with the Nb_2O_5-coated TiO_2, compared with that without the Nb_2O_5.

The electron diffusion length (L_n) is a useful tool to reflect the electron collection efficiency (η_c) is as shown in Fig 5(c). Typical photocurrent and photovoltage transients from the SLIM-PCV measurements for DSSCs are given Table 2. L_n values were increased with increasing Nb_2O_5 coating, implying that electron collection is efficient with increasing the Nb_2O_5 coating. These results agree to the variation in current density of the corresponding devices. The electron lifetime (τ_e) values obtained from photovoltage transient shows that increased τ_e values with increasing the Nb_2O_5 coating and results agree with variation in photovoltage

Table 2. SLIM-PCV analysis at different coating of Nb_2O_5 on TiO_2 electrode.

Coating times of Nb_2O_5	D(cm^2/s)Electron diffusion coefficient	τ_e(s)Electron lifetime	L(μm)Electron diffusion length
Untreated	3.610E-07	0.0439	1.2589
1 time	3.750E-07	0.0524	1.4022
3 times	3.916E-07	0.0607	1.5411

values of the corresponding devices. Nb-doping has been reported to increase the possibility of recombination of electron-hole pair by generating new recombination centers and/or promoting band-to-band transition [37, 38]. In this study, however, the carrier recombination is suppressed in Nb_2O_5 coating photoanodes based on EIS and SLIM-PCV measurement. The beneficial effect of Nb_2O_5 coating could be related to the dynamic perspective. In other words, Nb_2O_5 coating could facilitate the electron transport and collection, which accounts for the enhanced lifetime.

4. Conclusions

The effect of 1 and 3 times Nb_2O_5 coating on the performance of dye-sensitized solar cells have studied successfully. With a dip-coating method, Nb_2O_5 energy barrier layer can be deposited successfully on TiO_2 photoanode. Nb_2O_5 with the appropriate thickness not only blocks the backward transfer of electrons, but also accelerates its forward transfer. An excessively thick layer of Nb_2O_5 prevents the transfer of photo-generated electrons to the TiO_2 photoanode because of the low conductivity of Nb_2O_5. As a result, the optimized Nb_2O_5/ TiO_2 photoanode exhibits a higher η value, which is better than the bare TiO_2 photoanode. The increased charge transfer could be one of the reasons for improved current densities as evidenced from electrochemical impedance and SLIM-PCV analysis.

Acknowledgments

This work was supported by the 2013 Yeungnam University Research Grant, and also supported by "Human Resources Program in Energy Technology" of the Korea Institute of Energy Technology Evaluation and planning (KETEP), granted financial resource from the Ministry of Trade, Industry & Energy, Republic of Korea. (No. 20154030200760).

References

[1] Mei, X., Cho, S. J., Fan, B. (2010). *Nanotechnology*, *21*, 395202.
[2] Bella, F., Gerbaldi, C., Barolob, C., Gratzel, M. (2015). *Chem. Soc. Rev.*, *44*, 3431.
[3] Zhang, W., Zhu, R., Ke, L., Liu, X., Liu, B., Ramakrishna, S. (2010). *Small*, *6*, 2176.
[4] Poudel, P., Qiao, Q. (2012). *Nanoscale*, *4*, 2826.
[5] Wu, M. X., Lin, X., Wang, T. H., Qiu, J. S., Ma, T. L. (2011). *Energy Environ. Sci.*, *4*, 2308.
[6] Shao, F., Sun, J., Gao, L., Yang, S., Luo, J. (2010). *J. Phys. Chem. C*, *115*, 1819.
[7] Joshi, P., Xie, Y., Ropp, M., Galipeau, D., Bailey, S., Qiao, Q. Q. (2009). *Energy Environ. Sci.*, *2*, 426.
[8] Wu, J., Lan, Z., Lin, J., Huang, M., Huang, Y., Fan, L., Luo, G. (2015). *Chem. Rev*, *115*, 2136.
[9] Poudel, P., Zhang, L., Joshi, P., Venkatesan, S., Fong, H., Qiao, Q. (2012). *Nanoscale*, *4*, 4726.
[10] Joshi, P., Zhou, Z., Poudel, P., Thapa, A., Wu, X.-F., Qiao, Q. (2012). *Nanoscale*, *4*, 5659.
[11] O'Regan, B., Gratzel, M. (1991). *Nature*, *353*, 347.
[12] Kalyanasundaram, K., Gratzel, M. (1998). *Coord. Chem. Rev.*, *77*, 347.
[13] Hagfeldt, A., Lindquist, S. E., Gratzel, M. (1994). *Sol. Energy Mater. Sol. Cells*, *32*, 245.
[14] Tachibana, Y., Moser, J. E., Gratzel, M., Klug, D., Durrant, J. R. (1996). *J. Phys. Chem. B*, *100*, 20056.

[15] Bedja, I., Hotchandani, S., Kamat, P. V. (1997). *Ber. Bunsen-Ges. Phys.Chem. Chem. Phys.*, *101*, 1651.
[16] Nasr, C., Kamat, P. V., Hotchandani, S. (1997). *J. Electroanal. Chem.*, *420*, 201.
[17] Pichot, F., Gregg, B. A. (2000). *J. Phys. Chem. B*, *104*, 6.
[18] Prasittichai, C., Hupp, J. T. (2010). *J. Phys. Chem. Lett.*, *1*, 1611.
[19] Palomares, E., Clifford, J. N., Haque, S. A., Lutz, T., Durrant, J.R. (2003). *J. Am. Chem. Soc.*, *125*, 475.
[20] Barea, E., Xu, X. Q., Gonzalez-Pedro, V., Ripolles-Sanchis, T., Fabregat-Santiago, F., Bisquert, J. (2011). *Energy Environ. Sci.*, *4*, 3414.
[21] Ueno, S., Fujihara, S. (2011). *Electrochim. Acta*, *56*, 2906.
[22] Yang, M., Kim, D., Jha, H., Lee, K., Paul, J., Schmuki, P. (2011). *Chem. Commun.*, *47*, 2032.
[23] Ahn, K. S., Kang, M. S., Lee, J. K., Shin, B. C., Lee, J. W. (2006). *Appl. Phys. Lett.*, *89*, 013103.
[24] Lin, C., Tsai, F. Y., Lee, M. H., Lee, C. H., Tien, T. C., Wang, L.P., Tsai, S. Y. (2009). *J. Mater. Chem.*, *19*, 2999.
[25] Makinen, V., Honkala, K., Hakkinen, H. (2011). *J. Phys. Chem. C*, *115*, 9250.
[26] Law, M., Greene, L. E., Radenovic, A., Kuykendall, T., Liphardt, J., Yang, P. D. J. (2006). *Phys. Chem. B*, *110*, 22652.
[27] Lin, C., Tsai, F. Y., Lee, M. H., Lee, C. H., Tien, T. C., Wang, L.P., Tsai, S. Y. (2009). *J. Mater. Chem.*, *19*, 2999.
[28] O'Regan, B., Lenzmann, F. (2004). *J. Phys. Chem. B*, *108*, 4342.
[29] Snaith, H. J., Humphry-Baker, R., Chen, P., Cesar, I., Grätzel, M. (2008). *Nanotechnology*, *19*, 424003.
[30] Wang, Z. R., Ran, S. H., Liu, B., Chen, D., Shen, G. Z. (2012). *Nanoscale*, *4*, 3350.
[31] Halme, J., Vahermaa, P., Miettunen, K., Lund, P. (2010). *Adv. Mater.*, *22*, E210.
[32] Halme, J., Boschloo, G., Hagfeldt, A., Lund, P. (2008). *J. Phys.Chem. C*, *112*, 5623.
[33] Adachi, M., Sakamoto, M., Jiu, J. T., Ogata, Y., Isoda, S. (2006). *J. Phys. Chem. B*, *110*, 13872.
[34] Palomares, E., Clifford, J. N., Haque, S. A., Lutz, T., Durrant, J. R. (2003). *J. Am. Chem. Soc.*, *125*, 475.
[35] Yang, M., Kim, D., Jha, H., Lee, K., Paul, J., Schmuki, P. (2011). *Chem. Commun.*, *47*, 2032–2034.
[36] Furubayashi, Y., Yamada, N., Hirose, Y., Yamamoto, Y., Otani, M., Hitosugi, T., Shimada, T., Hasegawa, T. (2007). *J. Appl. Phys.*, *101*, 093705.
[37] Emeline, A.V., Furubayashi, Y., Zhang, X.T., Jin, M., Murakami, T., Fujishima, A. (2005). *J. Phys. Chem. B*, *109*, 24441.
[38] Mattsson, A., Leideborg, M., Larsson, K., Westin, G., Osterlund, L. (2006). *J. Phys. Chem. B*, *110*, 1210.